EFFECT OF MELTER-FEED-MAKEUP ON VITRIFICATION PROCESS

Prepared for the U.S. Department of Energy
Assistant Secretary for Environmental Management

Contractor for the U.S. Department of Energy
under Contract DE-AC06-08RL14788

CH2MHILL
Plateau Remediation Company

P.O. Box 1600
Richland, Washington 99352

Approved for Public Release;
Further Dissemination Unlimited

EFFECT OF MELTER-FEED-MAKEUP ON VITRIFICATION PROCESS

P. R. Hrma
Pacific Northwest National Laboratory

A. A. Kruger
Department of Energy - Office of River Protection

M. J. Schweiger
C. J. Humrickhouse
J. A. Moody
R. M. Tate
N. E. TeGrotenhuis
B. M. Arrigoni
C. P. Rodriguez
Pacific Northwest National Laboratory

Prepared for the U.S. Department of Energy
Assistant Secretary for Environmental Management

CH2MHILL
Plateau Remediation Company

P.O. Box 1600
Richland, Washington

Approved for Public Release;
Further Dissemination Unlimited

Release Approval   Date 09/10/2009

LEGAL DISCLAIMER

EFFECT OF MELTER-FEED-MAKEUP ON VITRIFICATION PROCESS

P Hrma, MJ Schweiger, CJ Humrickhouse, JA Moody, RM Tate, NE TeGrotenhuis, BM Arrigoni, CP Rodriguez

Pacific Northwest National Laboratory, Richland, Washington; pavel.hrma@pnl.gov

Increasing the rate of glass processing in the Hanford Tank Waste Treatment and Immobilization Plant (WTP) will allow shortening the life cycle of waste cleanup at the Hanford Site. While the WTP melters have approached the limit of increasing the rate of melting by enhancing the heat transfer rate from molten glass to the cold cap, a substantial improvement can still be achieved by accelerating the feed-to-glass conversion kinetics. This study investigates how the feed-to-glass conversion process responds to the feed makeup. By identifying the means of control of primary foam formation and silica grain dissolution, it provides data needed for a meaningful and economical design of large-scale experiments aimed at achieving faster melting.

INTRODUCTION

Understanding the relationship between melter-feed makeup and the feed-to-glass conversion process will help accelerate the rate of glass processing in the Hanford Tank Waste Treatment and Immobilization Plant (WTP). The mission of the WTP is to vitrify the Hanford nuclear waste. This will be done in continuous all-electric melters that contain a pool of molten glass in which the temperature is kept constant by passing electrical current through it. Feed is introduced into the melter from above in the form of water slurry. As water evaporates, a crust of dry feed, called the cold cap, floats on the melt pool and turns into melt at its bottom surface.

In the continuous glass melter, the rate of processing is jointly controlled by the rate of heat-transfer from molten glass to the cold cap and by the kinetics of various chemical

reactions and phase transitions within the cold cap (Hrma, 1990). Advanced melters that have been developed for the WTP have reached a level of heat transfer at which the rate of melting is controlled mainly by the conversion kinetics within the cold cap (Matlak et al., 2007a; Chapman, 2004), which is the main focus of this study.

The reactions within the cold cap proceed as the feed moves from the top, where slurry is fed onto its surface, to the bottom, where the feed becomes molten glass (Hrma, 1982). To simulate these conditions in the laboratory as closely as possible, feeds were heated at a rate of 5°C/min rather than using isothermal heat treatments. Feed conversion reactions advance while the temperature is increasing in a similar manner in a crucible as when the feed moves through a steep temperature gradient that exists in the cold cap.

The feed makeup affects feed conversion parameters, such as feed density, heat conductivity, rate of conversion, and conversion heat, through the interplay of various processes that take place within a cold cap and ultimately determine its rate of melting.

Feed density can vary extensively within the cold cap but to a great extent depends upon the extent of gas entrapment in the form of bubbles and cavities, known as primary foam, found in the lower layer of the cold cap. The primary foam develops when there is an overlap between the evolution of gases and the formation of connected glass-forming melt (Kim and Hrma, 1990; Kim and Hrma, 1991).

The main factors that control the feed reactivity and the extent of gas entrapment in the feed are the nature of inorganic salts (nitrates and carbonates) and the size of silica particles. A powerful source of internal heat within the cold cap can be provided through exothermic reactions of carbohydrates, such as sucrose or cellulose, with oxyanionic salts, especially nitrates and nitrites (Bickford et al., 1990; Elliott et al., 1989; Josephs and Stone, 2001, Lambert et al. 2001; Smith at al. 1995).

Melter feed is a mixture of many diverse components that respond to heating in a complex manner (Hrma et al. 2002; Izak et al., 2001; Smith et al. 2004). Because of this complexity of the cold-cap process, it is impossible to determine the rate of melting in a large continuous melter with laboratory crucible experiments alone. Nevertheless, laboratory studies provide insight into the feed conversion process that can guide melter experiments to obtain the relationship between the feed-makeup parameters and the rate of melting in a well focused, timely, and economic manner.

The aim of this laboratory study was to investigate how the melter-feed conversion process responds to changes in the feed makeup. The ultimate objective is to provide information for preparation of feeds designed for accelerating the rate of melting in continuous melters.

EXPERIMENTAL

Various methods of testing and analysis were used to examine these parameters. Flux migration testing (Hrma et al., 2007) was conducted to verify that molten salts are not likely to migrate out of the cold cap. Differential thermal analysis-thermal gravimetric analysis (DTA-TGA), X-ray diffraction (XRD), and scanning electron microscopy-energy-dispersive spectroscopy (SEM-EDS) identified the main feed reactions. Visual examination and optical microscopy of crucible melts and photographic recording of feed pellets and loose batches in quartz-glass crucibles were employed for detailed characterization of volume changes associated with the conversion process. Finally, temperature-field-evolution monitoring measured a temperature gradient, thus allowing

us to calculate the thermal conductivity of feed and providing a step towards understanding heat transfer in an actual cold-cap situation.

This study was performed with the high-level waste (HLW) feeds previously used in melter experiments conducted at the Vitreous State Laboratory (VSL): the baseline (BL) feed with the processing rate of 42 kg/m^2/h and a slow-melting (23 kg/m^2/h) Al-Na feed (Matlack et al., 2007a; 2007b; 2007c). The slurry feeds were dried before testing. Table 1 displays the feed and glass compositions.

To make a valid assessment of feed reactivity, great care was made to simulate not only the chemical composition of the waste in terms of oxides, but also its physical form and its chemical form in terms of compounds (e.g., oxides versus hydroxides or nitrates). Therefore, the base Al-limited feed, denoted as A0 feed (Table 2), was formulated to produce a glass designed at VSL but with chemicals selected to simulate the waste as truly as possible and with easy-reacting additives.

RESULTS
Migration tests

No migration of molten inorganic salt within the feeds was detected. This low mobility of molten salt within the HLW feeds can be attributed to the large specific surface area of the feed solids that immobilizes the molten salt via wetting the particles (Hrma et al., 1991). Hence, molten salt is unlikely to migrate in the HLW melter feeds.

Visual examination of quenched samples (Figure 1)

A sample of the BL feed heated in ceramic crucibles became sintered at 600°C; a sample of the Al-Na feed sintered at 700°C. Both feeds swelled with the primary foam. Bubbles gradually coalesced to larger cavities that were no longer seen in the BL sample at 1000°C, but bubbles still prevailed at this temperature in the Al-Na sample, obviously as a result of higher viscosity of the Al-Na glass melt.
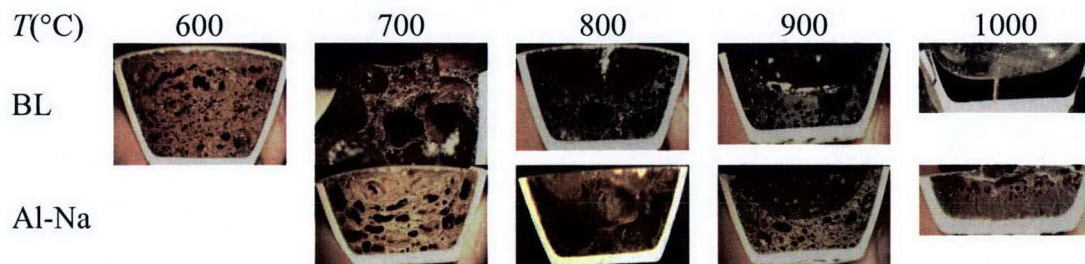

FIGURE 1. Cross-sections of feed samples (BL and Al-Na) heated at 5°C/min to temperatures from 600 to 1000°C

Glass	BL	Al-Na	Feed	BL	Al-Na
Al_2O_3	0.0529	0.2134	Al_2O_3	0.0529	0.2134
As_2O_5	0.0019		As_2O_3	0.0019	
B_2O_3	0.0939	0.1836	H_3BO_3		0.3262
BaO	0.0000	0.0003	$Na_2B_4O_7$	0.5428	
Bi_2O_3	0.0000	0.0116	$BaCO_3$		0.0004
CaO	0.0030	0.0072	Bi_2O_3		0.0116
CdO	0.0000	0.0001	CaO		0.0072
Cl	0.0011		$CaCO_3$	0.0054	
Cr_2O_3	0.0008	0.0071	CdO		0.0001
Cs_2O	0.0005		NaCl	0.0018	
CuO	0.0004		Cr_2O_3	0.0008	0.0071
F	0.0000	0.0023	CsOH	0.0005	
Fe_2O_3	0.1259	0.0281	CuO	0.0004	
I	0.0010		NaF		0.0050
K_2O	0.0000	0.0066	FeO_3H_3	0.1672	0.0072
La_2O_3	0.0024		NaI	0.0012	
Li_2O	0.0301	0.0357	KNO_3		0.0142
MgO	0.0117	0.0022	LaO_3H_3	0.0021	
MnO	0.0400		Li_2CO_3	0.0744	0.0884
Na_2O	0.1184	0.1271	MgO	0.0169	0.0022
Nd_2O_3	0.0015		MnO_2	0.0490	
NiO	0.0017	0.0010	NaOH		0.1066
P_2O_5	0.0009	0.0202	Nd_2O_3	0.0015	
PbO	0.0014	0.0009	NiO_2H_2	0.0021	0.0012
Sb_2O_3	0.0026		$FePO_4$	0.0019	0.0429
SeO_2	0.0037		PbO	0.0014	0.0009
SiO_2	0.4704	0.3457	Sb_2O_3	0.0026	
SO_3	0.0000	0.0022	SeO_2	0.0037	
SrO	0.0092		SiO_2	0.4704	0.3457
TiO_2	0.0014	0.0017	Na_2SO_4		0.0038
ZnO	0.0207	0.0018	$SrCO_3$	0.0131	
ZrO_2	0.0026	0.0012	TiO_2	0.0014	0.0017
CO_3	0.0129	0.0056	ZnO	0.0207	0.0018
NO_2	3.3×10^{-5}	0.0024	ZrO_4H_4	0.0034	0.0016
NO_3	0.0022	0.0094	Na_2CO_3	0.0556	0.0212
TOC	7.2×10^{-5}	2.4×10^{-4}	$NaNO_2$	0.0000	0.0150
			$NaNO_3$	0.0030	0.0548

TABLE 2.
Composition of Al-Limited Glass (Matlack et al., 2007a) and Feed Composition to Make 500 g of Simplified Al-Limited (A0) Glass. Oxides and halides are in mass fractions; carbonate, nitrite, nitrate, and total organic carbon (TOC) are listed as mass per a mass unit of glass.

	Al-Limited		Mass (g)
Al_2O_3	0.2397	$Al(OH)_3$	183.74
B_2O_3	0.1519	H_3BO_3	134.91
Bi_2O_3	0.0114	$Bi(OH)_3$	6.40
CaO	0.0608	CaO	30.39
Cr_2O_3	0.0052	Na_2CrO_4	5.57
F	0.0067	NaF	7.39
Fe_2O_3	0.0590	$Fe(OH)_3$	36.91
K_2O	0.0014	KNO_3	1.52
Li_2O	0.0357	Li_2CO_3	44.15
MgO	0.0012	$Mg(OH)_2$	0.85
Na_2O	0.0958	NaOH	48.53
NiO	0.0040	$NiCO_3$	3.18
P_2O_5	0.0105	$Fe(H_2PO_2)_3$	6.21
PbO	0.0041	$Pb(NO_3)_2$	3.04
SiO_2	0.3050	SiO_2	152.53
SO_3	0.0020	Na_2SO_4	1.78
ZnO	0.0008	$Zn(NO_3)_2·4H_2O$	1.33
ZrO_2	0.0039	$Zr(OH)_4·0.6H_2O$	2.74
NO_2	0.0023	$NaNO_2$	1.69
NO_3	0.0090	$NaNO_3$	2.46
TOC	$2.3×10^{-4}$	$Na_2C_2O_4·3H_2O$	0.88

Temperature field evolution

The temperature-field-evolution was measured in large silica crucibles (200 mm tall and 135 mm in diameter) equipped with a battery of thermocouples. The furnace temperature increased at 5°C/min. At feed temperatures between 300 and 600°C, the horizontal temperature distribution in the feed was close to parabolic. The heat flux was calculated using the measured temperature difference across the crucible wall (the heat conductivity of the crucible material was 1.3 $W/m^2/K$). Based on the temperature distribution within the feed (Figure 2), the heat conductivity of the feed was estimated for the temperature interval from 300 to 600°C as 1.28±0.17 $W/m^2/K$ for the BL and 1.99±0.82 $W/m^2/K$ for the Al-Na feed. Thus, no significant difference was found between the feeds, and the heat conductivity was virtually independent of temperature. Above 700°C, large cavities formed under the cold portion of the feed and the temperature gradient disappeared.

Feed expansion

To observe volume changes of feeds, pellets (Figure 3) and loose batches in silica-glass crucibles were heated at 5°C/min. Photographs were taken and the photos were evaluated with Photoshop software. The major difference between the fast-melting BL feed and the slow-melting Al-Na feed was that the latter expanded at a higher

temperature, starting at ~700°C and culminating at ~900°C, as compared to the range of ~600°C to ~800°C of the former (Figure 4).
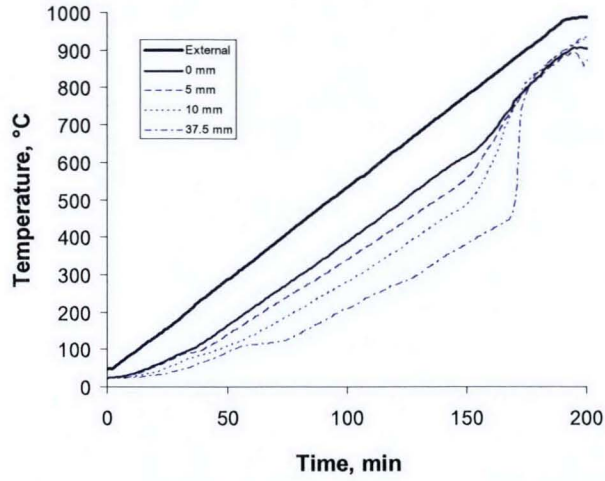

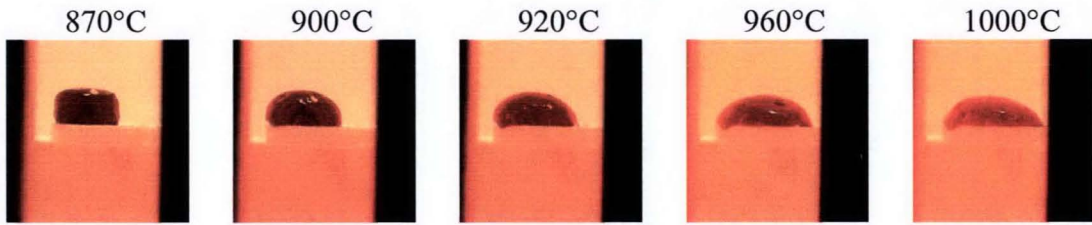FIGURE 2. Temperature versus time and
distance from crucible wall (legend) for BL feed.

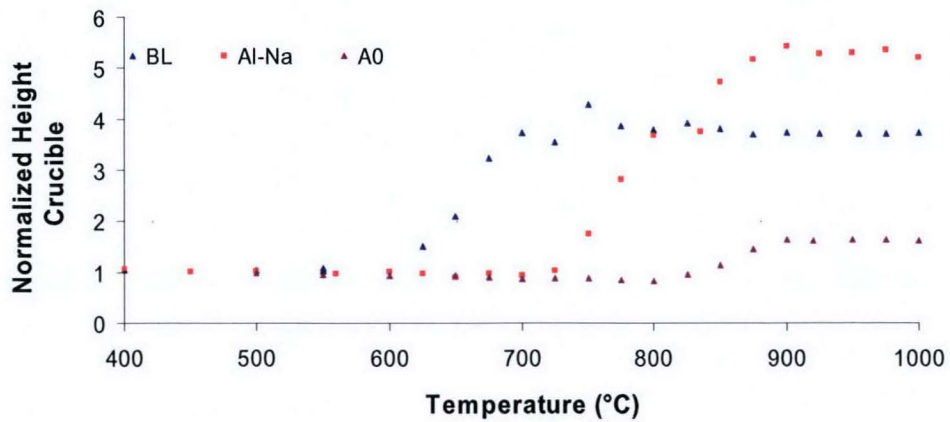FIGURE 3. Photographic images of feed A0 pellets in response to heating at 5°C/min.

FIGURE 4. Normalized feed height versus temperature for BL, Al-Na,
and A0 feeds placed in silica-glass crucible.

XRD

According to XRD results, silica began to react with feed fluxes at ~400°C. Only a small silica residue was found at 900°C and none at 1000°C in both BL and Al-Na feeds. Also, in A0 feed (with crushed quartz of 75-μm grain size), the solid silica was gone when the temperature approached 1000°C.

Several crystalline phases other than silica were detected in feeds using XRD. Hematite formed from amorphous iron oxyhydrate. Spinel formed from hematite starting at 500°C and peaked just above 600°C. Hematite completely dissolved below 800°C. Dissolving spinel remained in the glass even at 1000°C. In the Al-Na feed, nepheline and sodium salts-containing aluminosilicates appeared at temperatures above 400°C and were gone by 900°C.

SEM-EDS

In the BL feed at 600°C, SEM-EDS confirmed the presence of the glass phase, hematite [or possibly aegirine ($NaFeSi_2O_6$)], and spinel (probably hausmannite, Mn_3O_4, or hetaerolite $ZnMnO_4$), as well as dissolving particles of silica. At 700°C, apart from glass phase and dissolving silica particles, the patterns of spinel suggested hausmannite (Mn_3O_4) and franklinite $(Fe,Mn,Zn)(Fe,Mn)_2O_4$. Corundum was also detected. At 800°C, various forms of spinel were indicated by EDS: from hausmanite-franklinite solid solution; magnetite-jacobsite-trevorite ($MnFe_2O_4$-$NiFe_2O_4$) was also likely to form (Figure 5). At 900°C, the feed turned mostly to glass containing submicron crystals of spinel and silica residues. Silica was gone at 1000°C while spinel $(Ni,Fe,Mg,Mn)(Fe,Cr)_2O_4$ was surviving.

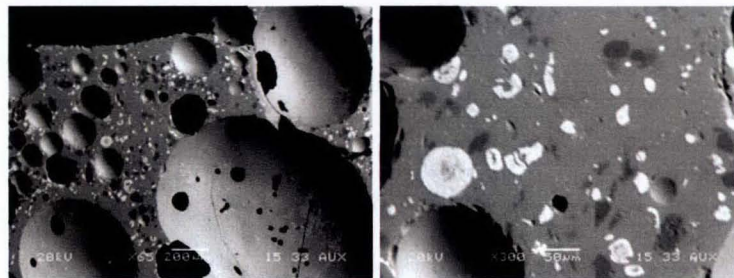FIGURE 5. SEM images of BL feed heat-treated at 5°C/min to 800°C. The white round object (right) is spinel, most likely a hausmanite-franklinite solid solution. The dark-gray rounded objects are dissolving silica grains.

In the Al-Na feed, inclusions of phosphate glass were suspected at 700°C. Particles of corundum, nepheline, and eskolaite (Cr_2O_3) or chromate (Na_2CrO_4) were clearly detected. Nepheline, needles of calcium phosphate, and spherolites of eskolaite were seen at 800°C. At 900°C, most of the sample was a connected amorphous phase containing rounded silica particles, spinel, and nepheline (Figure 6). At 1000°C, tiny crystals of chromite ($FeCr_2O_4$) were detected on the surfaces of bubbles.
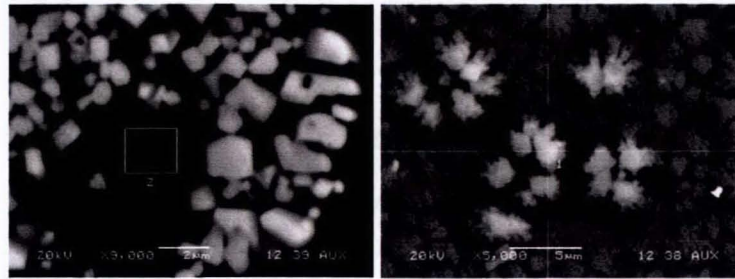
FIGURE 6. SEM images of Al-Na feed heat-treated at 5°C/min to 900°C. Spinel forms a cluster of small white crystals (left). The white and gray irregular objects are nepheline (right).

DTA-TGA

These tests showed that the major mass loss begins in feeds at ~150°C and continues to 600°C; above 600°C, it proceeds at a rather slow rate.

DISCUSSION

As mentioned in the introduction, the melter feed is charged into the melter from above and floats on the melt pool in the form of a cold cap that turns into melt at its bottom surface. From the point of view of an external observer, the temperature, velocity, and conversion extent of feed within the cold cap are distributed along a vertical coordinate. Ideally, when a steady state is established, this distribution is time-independent and represents the temporal history of the feed passing through the cold cap. The 5°C/min temperature-increase rate of feed samples in laboratory crucibles that we used in this study roughly simulated a typical temperature history that feed experiences within the cold cap.

Somewhat simplifying, the cold cap consists of two layers: the upper layer of granular solids soaked with low-viscosity molten salts and the lower layer of primary foam of glass-forming melt and dispersed solid residues, mainly silica and spinel. Most of the conversion reactions occur in the upper layer. It is there where the chemically bonded water is released, where oxyionic salts melt and react with organics and with solids, and where the first borate and silicate melts form.

In the lower layer, the borosilicate glass-forming melt becomes connected. Gases generated in this layer are trapped as primary foam. This foam collapses when enough gas is evolved to cause the melt films separating the bubbles to break. A distinction needs to be made between primary and secondary foam. Secondary foam is produced by redox reactions (known as fining reactions in commercial technology) at temperatures >900°C. This foam affects the rate of melting, but is not a part of the cold cap.

Most of the heat for feed-to-glass conversion is consumed in the upper layer of the cold cap. Enough heat must be conducted to evaporate water, to heat up the feed components, to provide energy for feed reactions, and to heat up feed gases, including steam. This heat is transferred from molten glass through the primary-foam layer. The thickness and the effective heat conductivity of the primary-foam layer in the melter are unknown. Both depend on the interaction between the internal gas-phase source and the glass-forming melt.

At the cold cap bottom, the feed is vitrified to the point at which it can be carried away by the circulation of currents within the melter. This happens after the melt viscosity becomes sufficiently low and the density sufficiently high so the bubbly melt no longer resists motion. The cold-cap bottom would effectively be above the temperature of maximum expansion, i.e., 800°C in the case of the BL feed and ~900°C in the case of Al-Na and A0 feeds. However, Al-Na feed expands three times as much as A0 feed (Figure 4). The overall melt density at the maximum expansion of Al-Na feed is 0.14 g/cm^3 and that of A0 feed 0.37 g/cm^3. Though significantly different, both densities are substantially lower than the melt density (~2.7 g/cm^3). Would this difference in densities affect the temperature of the cold-cap bottom and the rate of melting? The ultimate impact of the extent, even absence, of primary foam on the ease of melting is difficult to assess. A melter experiment can provide the answer.

CONCLUSION

Although it is not fully understood at this stage to what extent the decrease or avoidance of primary foam will affect the rate of melting, the present study identifies the means of control of primary foam formation. The approach developed in this study can provide quantitative data needed for a meaningful and economic design of large-scale experiments aimed at achieving faster melting. Moreover, mathematical models can now be developed that include the cold cap as a body with temperature and velocity fields rather than a mere mass source and heat sink with no vertical dimension.

ACKNOWLEDGMENTS

REFERENCES

Bickford DF, P Hrma, and BW Bowen II. 1990. "Control of Radioactive Waste Glass Melters: II, Residence Time and Melt Rate Limitations." *J. Am. Ceram. Soc.* 73:2903-2915.

Chapman C. 2004. *Investigation of Glass Bubbling and Increased Production Rate.* REP-RPP-069, Duratek, Inc., Columbia, Maryland.

Elliott ML, CC Chapman, LL Eyler, and DD Yasuda. 1989. *Preliminary Studies of Vitrification Rate Enhancement.* Pacific Northwest Laboratory, Richland, Washington.

Hrma P. 1982. "Thermodynamics of Batch melting." *Glastechn. Ber.* 55:138-150.

Hrma P. 1990. "Melting of Foaming Batches: Nuclear Waste Glass." *Glastech. Ber.* 63K:360-369.

Hrma P, CE Goles, and DD Yasuda. 1991. "Drainage of Primary Melt in a Glass Batch." *Ceram. Trans.* 23:361-367.

Hrma P, J Matyáš, and D-S Kim. 2002. "The Chemistry and Physics of Melter Cold Cap." In: *9th Biennial Int. Conf. On Nucl. And Hazardous Waste Management, Spectrum '02*, American Nuclear Society, CD-ROM.

Hrma P, LM Bagaasen, MJ Schweiger, MB Evans, BT Smith, BM Arrigoni, D-S Kim, CP Rodriguez, ST Yokuda, J Matyas, WC Buchmiller, AB Gallegos, A Fluegel. 2007. *Bulk Vitrification Performance Enhancement: Refractory Lining Protection Against Molten Salt Penetration.* PNNL-16773, Pacific Northwest National Laboratory, Richland, Washington.

Izak P, P Hrma, and MJ Schweiger. 2001. "Kinetics of Conversion of High-Level Waste to Glass." *ACS Symp. Series* 778:314-328.

Josephs JE and ME Stone. 2001. *Melt Rate Improvement for DWPF MB3: Sugar Addition Test.* WSRC-TR-2001-00158, Westinghouse Savannah River Company, Aiken, South Carolina.

Kim D-S and P Hrma. 1990. "Volume Changes During Batch to Glass Conversion." *Ceram. Bull.* 69[6]:1039-1043.

Kim D-S and P Hrma. 1991. "Foaming in Glass Melts Produced by Sodium Sulfate Decomposition under Isothermal Conditions." *J. Am. Ceram. Soc.* 74[3]:551-555.

Lambert DP, TH Lorier, DK Peeler, and ME Stone. 2001. *Melt Rate Improvement for DWPF MB3: Summary and Recommendations.* WSRC-TR-2001-00148, Westinghouse Savannah River Company, Aiken, South Carolina.

Matlack KS, H Gan, W Gong, IL Pegg, CC Chapman, and I Joseph. 2007a. *High Level Waste Vitrification System Improvements.* VSL-07R1010-1, Vitreous State Laboratory of the Catholic University of America, Washington, D.C.

Matlack KS, W Kot, W Gong, and IL Pegg. 2007b. *Small Scale Melter Testing of HLW Algorithm Glasses: Matrix 1 Tests.* VSL-07R1220-1, Vitreous State Laboratory of the Catholic University of America, Washington D.C.

Matlack KS, WK Kot, IL Pegg, and I Joseph. 2007c. *High Level Waste Glass Development Testing (Test Plan).* VSL-07T1360-1, Vitreous State Laboratory at the Catholic University of America, Washington D.C.

Smith PA, JD Vienna, and P Hrma. 1995. "The Effect of Melting Reactions on Laboratory-Scale Waste Vitrification." *J. Mat. Res.* 10[8]:2137-2149.

Smith ME, DH Miller, and TH Lorier. 2004. *Impact of Feed Preparation Acid Stoichiometry and Redox on Melt Rate for the SB3-Frit 418 Feed System.* WSRC-TR2004-00350, Savannah River National Laboratory, Aiken, South Carolina.